*J. Fluid Mech.* (1982), *vol.*
*Printed in Great Britain*



# Self-generation of organized waves in an impinging turbulent jet at low Mach number

BY DONALD ROCKWELL
AND ANDREAS SCHACHENMANN†

Department of Mechanical Engineering and Mechanics,
Lehigh University, Bethlehem, Pa. 18015, U.S.A.

(Received 7 May 1980 and in revised form 9 April 1981)

Self-generation of highly organized waves in a nominally turbulent jet at very low Mach number can arise from its impingement upon the downstream orifice of an axisymmetric cavity, having an impingement length much shorter than the corresponding acoustic wavelength. The oscillation frequencies are compatible with the resonant modes of a long pipe located upstream of the cavity and with jet-instability frequencies based on the column mode ($0{\cdot}3 \lesssim S_D \lesssim 0{\cdot}6$), as well as the near-field shear layer mode ($0{\cdot}016 \lesssim S_{\theta_0} \lesssim 0{\cdot}03$). Moreover, the frequency of the organized wave is constant from separation to impingement; consequently vortex pairing does not occur.

Within the cavity, the pressure amplitude associated with the organized wave is directly related to the phase difference between the organized velocity fluctuations at separation and impingement. Maximum pressure amplitude occurs when this phase difference, measured along the cavity (i.e. jet) centre-line, is $2n\pi$. Streamwise amplitude and phase distributions of the organized wave cannot be explained from purely hydrodynamic considerations; however, they can be effectively modelled by superposing contributions from hydrodynamic and acoustic waves. This aspect has important consequences for externally excited jets as well.

## 1. Introduction

Discrete tones and pressure fluctuations have been detected at low Mach number in a variety of configurations with nominally turbulent flow. Parker (1966) has observed coherent pressure fluctuations due to coupling of vortex shedding from the trailing edge of a flat plate with a resonant mode of the test section, subsequently studied by Cumpsty & Whitehead (1971) and Archibald (1975). Tam & Block (1978) and Elder (1978), as well as other investigators cited therein, have detected organized pressure fluctuations due to coupling of a turbulent shear layer past a cavity with a normal acoustic mode or Helmholtz mode of the cavity. Rockwell and Schachenmann (Rockwell & Schachenmann 1979; Schachenmann & Rockwell 1980) have reported self-generated oscillations of a cavity and a cavity–tailpipe combination due to accentuation of the cavity shear layer coherence by upstream organ-pipe modes and by Helmholtz resonance of the upstream settling chamber: Hill & Greene (1977) and Hasan & Hussain (1979) have observed discrete fluctuations of a finite-length sudden

† On leave from position of Research Engineer, Fluid Mechanics Laboratory, Sulzer Brothers, Winterthur, Switzerland.

expansion ('pipe collar') at the end of a pipe, due to coupling of the separated region in the expansion with the acoustic mode of the pipe.

The essential, and intriguing, feature of all of these self-generated oscillations is that the separated turbulent shear layer would appear to exhibit an inherent instability, enhanced by the presence of an adjacent acoustic resonator. In this regard, Rockwell (1977) and Tam & Block (1978) have shown that accounting for shear-layer instability in conceptually simple models of cavity oscillations yields predicted frequencies in reasonable agreement with measurements. Yet, in determining the criterion for oscillation at a given frequency, in these studies as well as in related investigations cited therein, it has been necessary to make certain critical assumptions, which emphasize the need for experimental insight. These assumptions include: spatial homogeneity of the unsteady shear layer near impingement ($x = L$ in figure 1) and, in some cases, near separation ($x = 0$ in figure 1) as well; existence of a certain phase relation between a line source and shear-layer deflection at impingement (Tam & Block 1978), or between integrated deflection of the shear layer and perturbations at separation (Rockwell 1977); and propagation of an unstable organized wave exhibiting exponential growth along the entire length of the cavity, describable by inviscid, quasiparallel-flow stability concepts.

Experimental investigations of the aforementioned impinging turbulent flows (cavity, pipe-collar) have typically been limited to single-point pressure or velocity measurements, with the objective of characterizing the oscillation frequency. However, two-point correlations (or their equivalent) of the unsteady shear-layer parameters, yielding streamwise distributions of phase and amplitude of the organized wave, are essential for a full understanding of the oscillation mechanism. Moreover, the fact that the oscillations of an impinging turbulent shear layer are self-generated suggests, among other features, a favourable phase difference (of organized wave velocity/pressure fluctuations) between separation and impingement. This aspect alone has been a source of conjecture and misunderstanding, even for simpler impinging flows involving unstable laminar shear layers (see the reviews of Rockwell 1982; Rockwell & Naudascher 1979; Karamcheti *et al.* 1969). Associated with this concept of a favourable phase difference between separation and impingement is the possibility of a finite delay time due to upstream propagating disturbances. This is underscored in the relatively high (subsonic) Mach number study of Ho & Nossier (1981), where the delay from impingement to separation was significant; accounting for it allowed determination of a 'phase-lock' criterion between waves at separation. In the present investigation, this upstream delay can be neglected, as the corresponding acoustic wavelength is much longer than the cavity length.

Although self-sustained oscillations of impinging turbulent jets at low Mach number have received very little attention, externally forced, non-impinging jets have been investigated by Crow & Champagne (1971), Moore (1977), Chan (1974) and Hussain & Zaman (1978*a*), who have all demonstrated the amplification of acoustically generated disturbances applied upstream of, or immediately downstream of, the nozzle exit. In general, the excitation Strouhal number (based on nozzle diameter) producing maximum disturbance amplification in the jet lies in the range $0{\cdot}3 \lesssim S_D \lesssim 0{\cdot}5$; these 'preferred modes' can be approximated using linear, inviscid stability theory (Michalke 1971; Plaschko 1979).

Though an underlying degree of organization of non-excited, non-impinging jets

has been suggested and/or characterized in various ways by Mollo-Christensen (1967), Ko & Davies (1971), Lau, Fisher & Fuchs (1972), and Davies & Yule (1975), extraction of these organized features requires conditional sampling as described for example by Maestrello & Fung (1979), and works reviewed therein. Recently, Kibens (1980), in a study of a turbulent jet formed at the end of a long pipe, states, on the basis of *non*-conditional autocorrelations, that the 'coherent energy levels in the shear layer and on the centre-line are low'. In contrast, the present investigation, which involves imposition of a finite length scale in the form of a downstream impingement orifice (see figure 1), yields strongly coherent oscillations that take the form of well-defined peaks in (non-conditional) spectra of the velocity and pressure fluctuations, provided the corresponding frequencies are compatible with resonant modes of the approach pipe.

These self-sustained oscillations can be represented by an 'organized wave'. It can be decomposed into two components: an acoustic contribution(s), having wavelength $\lambda_a$ and velocity $\tilde{u}_a$; and an instability (or hydrodynamic) contribution having wavelength $\lambda_i$ and velocity $\tilde{u}_i$. As will be shown, for the low Mach number ($M = U/\bar{c} \simeq 10^{-2}$) considered herein, $\lambda_a \gg \lambda_i$. The consequence of this limiting condition is that for length scales $L$ of interest in this study, where $L \simeq \lambda_i$, streamwise variations in amplitude and phase of the organized wave will be influenced primarily by those of the instability wave. Moreover, the pressure fluctuations associated with the acoustic wave(s) are of order $\rho\bar{c}\tilde{u}_a$ (see Ffowcs Williams 1969), where $\bar{c}$ is the speed of sound; those due to the instability (hydrodynamic) wave are of order $\rho U\tilde{u}_i$, where $U$ is mean velocity. For the low Mach numbers herein, the acoustic contribution can be expected to dominate the instability (hydrodynamic) contribution to the pressure of the organized wave in the regions of the flow where $\tilde{u}_i$ is sufficiently small relative to $\tilde{u}_a$. As will be shown, this is the case upstream of flow separation; downstream of separation (i.e. within the cavity of figure 1), $\tilde{u}_i$ is amplified, making it considerably larger relative to $\tilde{u}_a$.

In essence, the objectives of the present study of turbulent, self-excited oscillations are to: (i) relate streamwise differences in phase of the organized wave (between exit and entrance of the cavity) to the pressure amplitude within the cavity; (ii) characterize the streamwise evolution of the organized wave in the core of the jet; and (iii) examine the effects of relative amplitudes of the hydrodynamic and acoustic contributions to the organized wave.

## 2. Experimental system

The experimental apparatus, shown in figure 1, comprised an axisymmetric cavity preceded by a long pipe of length $l$ and diameter $D$, which insured a fully turbulent flow at the entrance of the cavity; it also acted as a long-wavelength resonator, enhancing the self-generated cavity oscillations. For this series of experiments, $D = 44{\cdot}45$ mm, $l/D = 82{\cdot}3$ and $1 \leqslant L/D \leqslant 2{\cdot}5$. The approach flow Reynolds number $Re_D (= U_0 D/\nu$, $U_0 \equiv$ centre-line velocity at pipe exit) was varied over the range of $1{\cdot}3 \times 10^4 \leqslant Re_D \leqslant 4 \times 10^4$. Mean velocity at the exit of the pipe was well-fitted with a power-law profile ($n = 6{\cdot}6$), agreeing well with the data of Laufer (1953) and giving a value of momentum thickness at the exit of the pipe, $\theta_0/D = 0{\cdot}05$; moreover, the distributions of background turbulence intensity were compatible with those measured by Laufer.

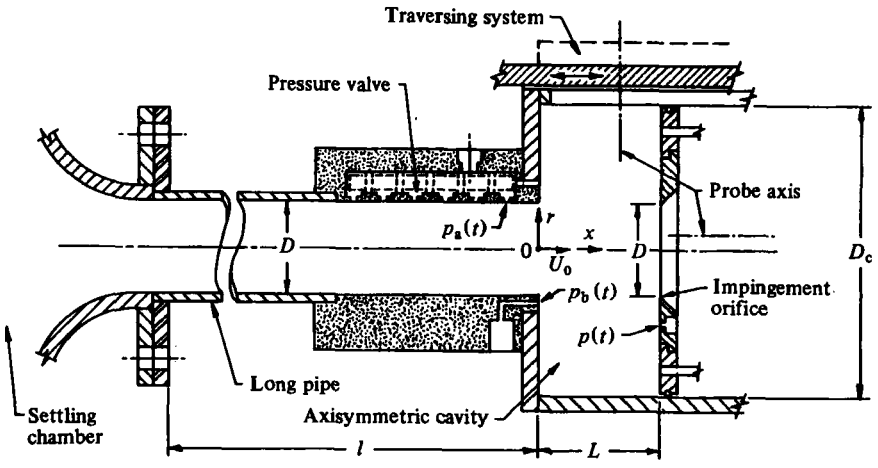


FIGURE 1. Schematic of experimental system comprising variable-length cavity preceded by long pipe.

Particularly important in the study of resonant-coupling phenomena is the no-flow frequency response of the settling-chamber–pipe–cavity system. Since coupling of the cavity oscillations with the pipe modes was of primary interest, it was essential to avoid Helmholtz-resonance contamination of the system response. Using a loudspeaker mounted on the side of the upstream settling chamber, the no-flow frequency response was determined at a nominal cavity length of $L = 90$ mm, and it was ascertained that the Helmholtz frequency of $H = 250$ Hz was above the $k = 3, 4, 5$ pipe modes (i.e. 137, 183, 227 Hz) of interest here; $k$ represents the 'organ-pipe' resonance mode with one end of the pipe open. There was a mild distortion of the $k = 5$ mode response by the Helmholtz resonance; therefore all detailed measurements of the self-induced oscillations were limited to the $k = 3, 4$ modes. Moreover, Helmholtz frequencies of the settling-chamber–pipe–loudspeaker combination (approximately 75 and 12 Hz for the two extreme locations of the loudspeaker adjustment chamber) were much lower than the oscillation frequencies characterized herein.

At the low frequencies of oscillations considered herein, the acoustic wavelength is very long ($\lambda_a/D \simeq 25$), and the orifice at the exit of the cavity has a reflection coefficient close to unity (Ronneberger 1967). Using the aforementioned loudspeaker as an excitation source (without mean flow $U$), the distribution of acoustic pressure was determined along the centre-line of the pipe-exit–cavity system; this distribution within the cavity, due to both downstream and upstream travelling waves (Skudrzyk 1971), served as the basis of approximation for acoustic-wave amplitudes employed in modelling the oscillation, to be discussed below.

Concerning the pressure-measurement stations shown in figure 1, pressure $\tilde{p}$ (at $x = L, r/R = 1{\cdot}1$) served as a reference signal in educing, via a lock-in amplifier, the amplitude and phase of the organized wave from the background turbulence. To determine the relative amplitudes of the acoustic $\tilde{u}_a$ and instability $\tilde{u}_i$ contributions to the organized wave $\tilde{u}$ near separation, $\tilde{p}_a$ was employed as a reference; at the frequencies of interest its amplitude and phase were within ten per cent of pressure $\tilde{p}_b$ (at $x = 0, r/R = 1{\cdot}11$), owing to the long acoustic wavelength. Two different microphone systems were used, a DISA 51F32 unit with a Bruel & Kjaer no. 4135, 6·35 mm

diameter microphone and a Hewlett–Packard no. 15118A, 12·5 mm diameter microphone. In all cases, the frequency response of each of the pressure-tap–microphone assemblies was tested using a reference microphone. Moreover, the theoretical method of Iberall (1950) was used as a further check. In all cases, there was negligible amplitude and phase distortion up to a frequency at least twice as high as the maximum frequency of interest.

Unsteady velocity measurements were carried out using two different hot-wire probe arrangements, with the axes of the probe holders oriented as shown in figure 1, in order to verify that probe-interference effects were insignificant. Both probes could be traversed in the $(x, r)$-plane, and the centre-line probe in the perpendicular plane as well, using two independent traversing systems. The system mounted on the cavity wall (at $r = R$), not shown in detail here, was constructed so that the $\frac{3}{16}$ in. slot through which the probe holder was translated was always completely sealed. Extensive checks were made on phase and amplitude distributions of the unsteady velocity field, using each probe independently; no probe interference was detectable.

Using an Ortec lock-in amplifier with a vector computer module, the organized wave was extracted from the background turbulence. The vector computer module of the lock-in amplifier gave the phase of the organized wave, leading to streamwise distributions of organized wave velocity $\tilde{u}$ and phase $\phi_{\tilde{u}}$. To acquire frequency spectra of the velocity and pressure fluctuations, the reference signal port of the lock-in amplifier was driven by a frequency ramp generator.

## 3. Overall features of oscillation

In order to determine the frequency of the predominant organized wave, and the degree of concentration of energy at the oscillation frequency, extensive spectra of velocity $u_{\rm rms}(f)/df$ and pressure $p_{\rm rms}(f)/df$ fluctuations were acquired. Typical spectra are given in figure 2. At two representative oscillation conditions, cases $(a)$ and $(b)$, there is a strong concentration of energy at a well-defined frequency. For case $(a)$, the self-generated cavity oscillation is coincident with the $k = 3$ pipe mode, and for case $(b)$, with the $k = 4$ mode (see figure 3 for operating conditions). At successively larger values of $r/R$, a single predominant peak was always evident, though the amplitude of the background turbulence became increasingly larger relative to the primary peak, requiring conditional sampling to extract the organized component. With regard to fluctuating pressure at impingement ($\tilde{p}$ in figure 1), corresponding spectra had shapes very similar to the velocity spectra of figure 2. Furthermore, the role of the impingement orifice is strikingly evident by comparing figure 2$(c)$ with figures 2$(a, b)$. In figure 2$(c)$, there is no evidence of strong coherence, suggesting that the upstream influence of the unsteady-flow impingement is a necessary ingredient in sustaining the organized wave. This observation is analogous to the study of Rockwell & Knisely (1979), involving enhancement of unstable *laminar* flow past a backward-facing step by insertion of a downstream impingement corner to form a cavity.

Shown in figure 2$(d)$ are representative pressure spectra taken at impingement ($\tilde{p}$ in figure 1), revealing the effect of the impingement length scale $L$ on the nature of the oscillation. At smaller values of $L$ there is no evidence of an organized oscillation; at $L/D = 0{\cdot}90$ the appearance of a peak in the pressure spectrum indicates existence of an organized wave; and at $L/D = 1{\cdot}00$ its amplitude has become very substantial.

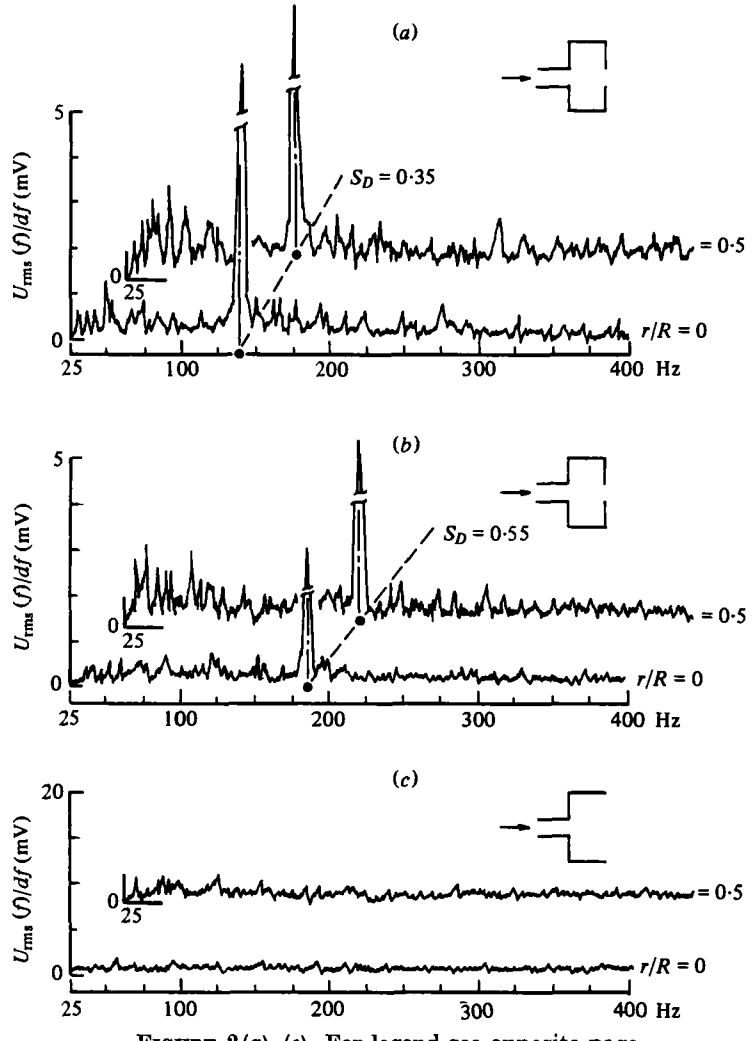


FIGURE 2(a)–(c). For legend see opposite page.

This variation of oscillation amplitude with length scale $L$ suggests that only when the jet shear-layer instability has a sufficiently long distance to amplify can a coherent, self-sustained oscillation occur. Such an observation is in accord with purely hydrodynamic oscillations of initially laminar flows, where a minimum length scale $L$ must be exceeded, thereby allowing adequate amplification of the unstable disturbance in the free shear layer (Rockwell & Naudascher 1979).

Frequencies of self-sustained oscillation (i.e. frequencies of the organized wave) determined from spectra of the sort shown in figures 2(*a*, *b*) are given in figure 3 for three different cavity lengths and a twofold range of centre-line velocity. Also shown are the theoretical (Skudrzyk 1971) and measured (loudspeaker excitation at no-through-flow) pipe modes. Clearly, the frequencies of oscillation are strongly influenced by the pipe modes, in contrast to the free (non-impinging) turbulent-jet investigation of Kibens (1980); when the boundary layer at the exit of his pipe became turbulent,

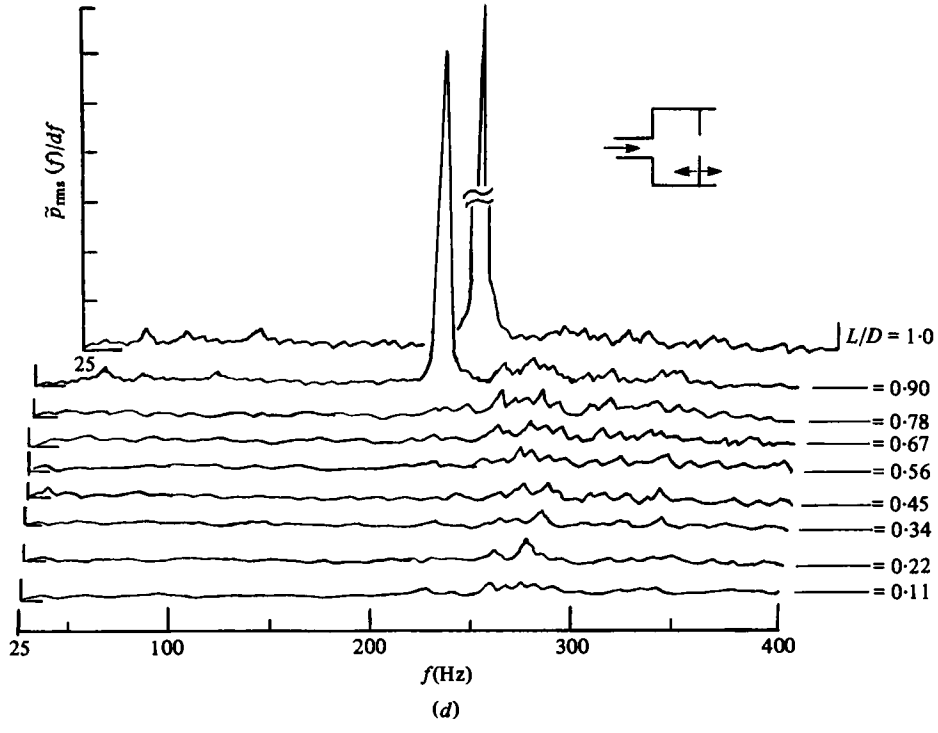


FIGURE 2. Typical spectra of velocity fluctuations $u_{rms}(f)/df$ and pressure fluctuations $p_{rms}(f)/df$ for representative oscillation conditions with impingement orifice and without orifice. (*a*) $L/D = 2$, $Re_{\theta_0} = 2{\cdot}6 \times 10^3$, $S_D = 0{\cdot}35$; (*b*) $L/D = 2$, $Re_{\theta_0} = 2{\cdot}2 \times 10^3$, $S_D = 0{\cdot}55$; (*c*) $L/D = \infty$ (no orifice), $Re_{\theta_0} = 2{\cdot}2 \times 10^3$; (*d*) $U_0 = 17{\cdot}1$ m/s; $Re_{\theta_0} = 2{\cdot}6 \times 10^3$.

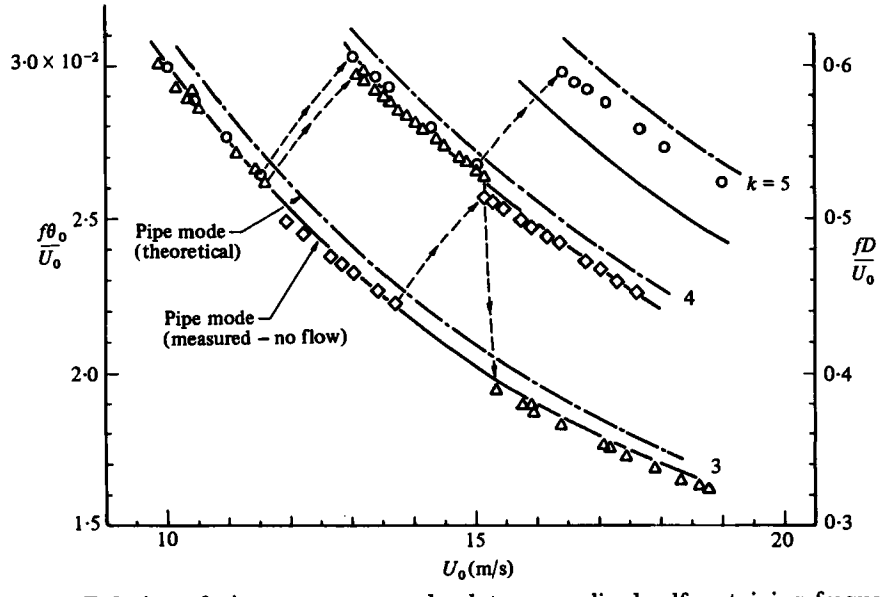


FIGURE 3. Relation of pipe resonance modes $k$ to normalized self-sustaining frequencies $f$ of organized wave for several values of cavity length $L$ over a range of centre-line velocity $U_0$. ○, $L/D = 1$; △, 2; ◇, 2·5.

a weakly coherent, but essentially constant Strouhal number ($S_D \simeq 0{\cdot}4$) persisted, uninfluenced by the pipe-resonance characteristics. Concerning the tendency of oscillations within the short cavity ($L/D = 1$) to remain at a relatively high value of $S_D$ (nominal $fD/U_0 \simeq 0{\cdot}55$) by means of successive jumps, it is in accord with the externally excited jet studies of Crow & Champagne (1971) and Chan (1974), who found predominance of higher $S_D$ at smaller streamwise length scales. The most striking feature of the data in figure 3 is that coherent oscillations occur only for those pipe modes ($k = 3, 4, 5$) corresponding to a certain band of dimensionless frequencies $f\theta_0/U_0$ and $fD/U_0$; lower ($k = 1, 2$) and higher ($k = 6, 7, \ldots$) modes are not selected by the self-sustained oscillation for the range of velocities considered. This preferred band of frequencies corresponds to the range of large-scale hydrodynamic instabilities of the jet within the cavity.

The fact that the frequencies of oscillation are compatible with those predicted for an axisymmetric jet using inviscid stability theory (Michalke 1971) is seen by examining the values of $S_\theta$: $0{\cdot}016 \lesssim S_{\theta_0} = f\theta_0/U \lesssim 0{\cdot}030$ for $R/\theta_0 = 10$ at $x = 0$. The amplification factor $-\alpha_i\theta_0$ has its maximum value, $-\alpha_i\theta_0)_{\max}$ at $S_{\theta_0} = 0{\cdot}019$; however, over this range of $S_{\theta_0}$, $-\alpha_i\theta_0 \gtrsim 0{\cdot}6\,(-\alpha_i\theta_0)_{\max}$. Accounting for the increase of momentum thickness in the downstream direction, as proposed by Michalke in analysing the data of Crow & Champagne (1971), the values of $S_\theta$ become $0{\cdot}024 \lesssim S_\theta \lesssim 0{\cdot}045$ for $R/\theta = 6{\cdot}5$ at $x/D = 1$. At $S_\theta = 0{\cdot}028$, $-\alpha_i\theta \simeq (-\alpha_i\theta)_{\max}$ for this lower value of $R/\theta$; again, over this range of $S_\theta$, there is always substantial amplification: $-\alpha_i\theta \gtrsim 0{\cdot}4\,(-\alpha_i\theta)_{\max}$. Thus, based on conditions at $x = 0$ (separation) or at $x = D$, the range of observed frequencies corresponds to disturbances experiencing very substantial amplification.

In addition, if the values of $S_D = fD/U_0$ of these oscillations are examined, further compatibility with observations of the most unstable frequencies (in the 'column mode') of turbulent jets is evidenced. For non-excited (Kibens 1980; Maestrello & Fung 1979; $0{\cdot}3 \lesssim S_D \lesssim 0{\cdot}5$), as well as externally excited (Crow & Champagne 1971; Chan 1974; $0{\cdot}3 \lesssim S_D \lesssim 0{\cdot}5$), free jets, there is general agreement with the range $0{\cdot}3 \lesssim S_D \lesssim 0{\cdot}6$ of figure 3.

Crow & Champagne (1971) and Kibens (1980) emphasize the importance of distinguishing between mechanisms characteristic of small-scale structures due to near-field instability of the usually thin, laminar, separating shear layer and its subharmonics, and large-scale structures associated with the 'column' instability of the jet, the former attaining the latter frequency through multiple vortex pairing (Kibens 1980). For the range of conditions corresponding to figure 3, extensive spectra showed persistence of the same predominant frequency of oscillation along the centre-line and in the shear layer as well, meaning that vortex pairing did not occur.

## 4. Streamwise phase differences of organized wave in cavity

In analogy with conceptual models for corresponding unstable laminar flows (Rockwell & Naudascher 1979), it may be presumed that the maximum pressure amplitude within the cavity is attained when some sort of favourable phase condition between fluctuations at separation ($x = 0$) and impingement ($x = L$) is satisfied. Regarding phase variations in the radial direction, it was found that the organized velocity fluctuation exhibits a core of essentially constant phase (i.e. $\partial\phi_{\tilde{u}}/\partial r$ very small for $r/R \lesssim 0{\cdot}5$). Taking advantage of this 'phase core', streamwise phase distributions

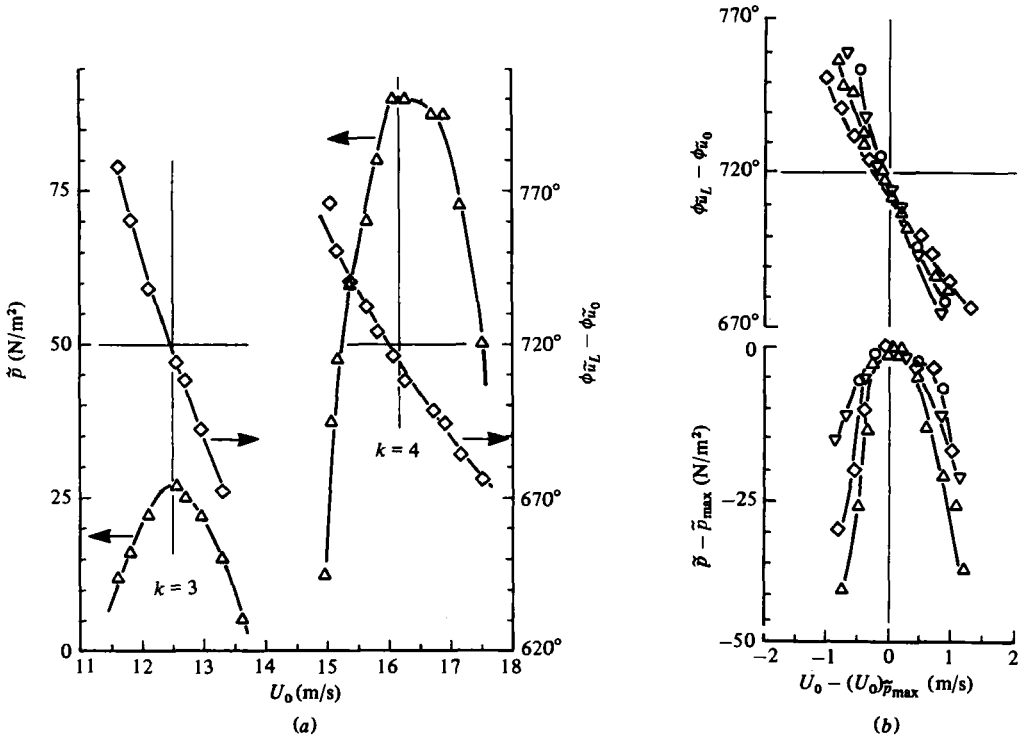


FIGURE 4 (*a*, *b*). For legend see p. 434.

were characterized along the centre-line of the cavity, rather than within the shear layer, where large transverse gradients of phase greatly complicate interpretation of streamwise variations. Variations of the phase difference $\phi_{\tilde{u}_L} - \phi_{\tilde{u}_0}$ of the streamwise component of the organized wave velocity between impingement and separation and of the amplitude of the organized pressure $\tilde{p}$ at impingement are given in figure 4 (*a*). Two complete stages of oscillation are evident; the maximum amplitude of each stage is reached when $\phi_{\tilde{u}_L} - \phi_{\tilde{u}_0} \simeq 4\pi$. Deviations in phase from this $2n\pi$ criterion result in corresponding decreases in amplitude of the organized pressure $\tilde{p}$. It is important that, for the representative data of figure 4 (*a*), pressure and velocity spectra showed no indication of a coherent oscillation for $14{\cdot}0 \lesssim U_0 \lesssim 14{\cdot}5$ m/s, underscoring the necessity of an acoustic resonator (i.e. organ pipe) in bringing out the inherent instability of the turbulent jet flow. This aspect, as well as typical spectra between pipe modes, are discussed by Schachenmann & Rockwell (1980).

Data of the sort given in figure 4 (*a*) were acquired for three values of cavity length $L$, corresponding to a 26-fold range of momentum thickness $\theta_0$. In addition, at each value of $L$, the velocity $U_0$ was varied over a two-fold range. All together, eight complete stages of oscillation were negotiated. (There are two complete stages in figure 4 (*a*).) Figure 4 (*b*) shows pressure amplitude referenced to its respective maximum ($\tilde{p} - \tilde{p}_{max}$) as a function of velocity deviation from the value of mean velocity giving maximum pressure amplitude ($U_0 - (U_0)_{\tilde{p}_{max}}$). It is clear that maximum pressure amplitude always occurs at $\phi_{\tilde{u}_L} - \phi_{\tilde{u}_0} = 2n\pi\,(n = 2)$. Similar correlations of maximum amplitude $\tilde{p}_{max}$ with phase difference $\phi_{\tilde{u}_L} - \phi_{\tilde{u}_0}$) for four other combinations of $L/D$ and $U_0$ also

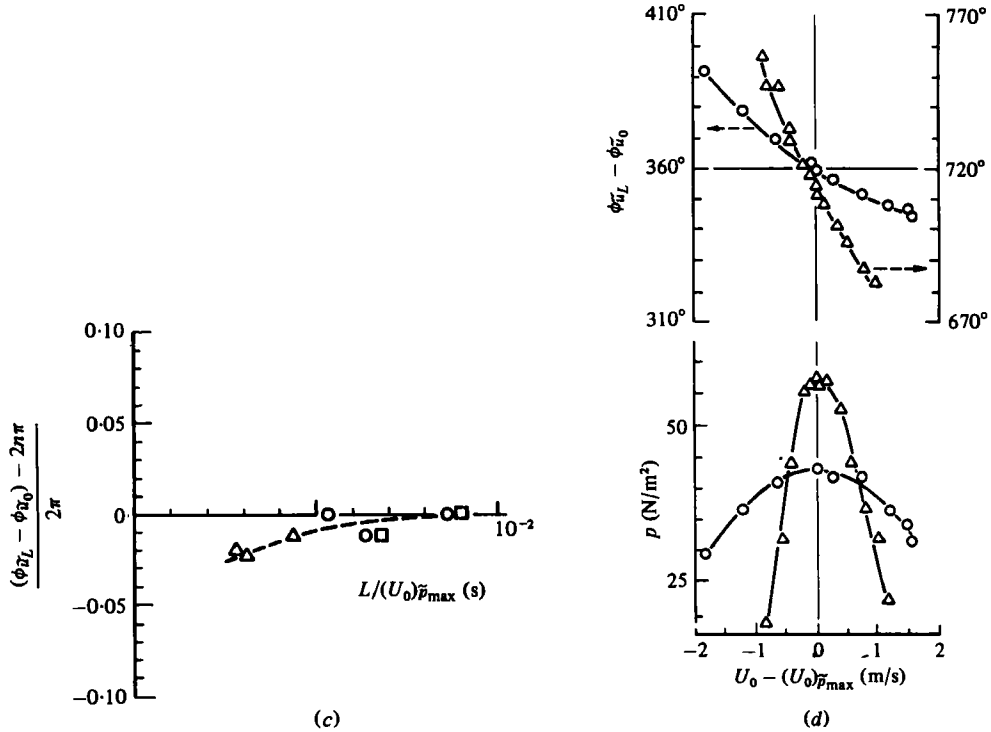


FIGURE 4. (*a*) Typical variations of organized pressure $p$ in cavity at impingement ($x = L$, $r/R = 1{\cdot}5$) (△) and phase difference $\phi_{\tilde{u}_L} - \phi_{\tilde{u}_0}$ of organized velocity wave $\tilde{u}$ along centre-line between impingement ($x = L$) and separation ($x = 0$) (◇) as functions of centre-line velocity $U_0$ at separation, $L/D = 2{\cdot}5$. (*b*) Variation of organized pressure amplitude $\tilde{p} - \tilde{p}_{max}$, and phase difference $\phi_{\tilde{u}_L} - \phi_{\tilde{u}_0}$ of organized wave velocity between separation ($x = 0$) and impingement ($x = L$) as a function of mean velocity deviation from that value giving maximum pressure response, $U_0 - (U_0)_{\tilde{p}_{max}}$. △, $L/D = 2$; $(U_0)_{\tilde{p}_{max}} = 14$ m/s; ○, 2, 10·6 m/s; ▽, 2·5, 12·5 m/s; ◇, 2·5, 16·3 m/s. (*c*) Normalized deviation of phase difference $\phi_{\tilde{u}_L} - \phi_{\tilde{u}_0}$ of organized wave velocity fluctuation as a function of ratio of cavity length $L$ to mean velocity giving maximum response $(U_0)_{\tilde{p}_{max}}$ for a range of cavity length and velocity. △, $L/D = 1$, $(\phi_{\tilde{u}_L} - \phi_{\tilde{u}_0})_{nominal} = 360°$; ○, 2, 360°, 720°; □, 2·5, 720°. (*d*) Comparison of organized pressure amplitude $\tilde{p}$ and phase difference $\phi_{\tilde{u}_L} - \phi_{\tilde{u}_0}$ as a function of mean velocity deviation from that value giving maximum pressure response, $U_0 - (U_0)_{\tilde{p}_{max}}$ for representative cases of $(\phi_{\tilde{u}_L} - \phi_{\tilde{u}_0}) = 360°$ and 720°. $L/D = 2{\cdot}0$. △, $(U_0)_{\tilde{p}_{max}} = 14{\cdot}4$ m/s. ○, 17·2 m/s.

showed the peak occurring at $2n\pi$ ($n = 1$); these cases of $n = 1$ tended to occur at smaller $L/D$ (see figure 4*d*).

The fact that the phase difference $\Delta\phi = \phi_{\tilde{u}_L} - \phi_{\tilde{u}_0}$ can be taken as $2n\pi$ is illustrated in figure 4(*c*). By using $2\pi$ as the normalization parameter for the vertical ordinate, deviations from $2n\pi$ are expressed in terms of one wavelength (corresponding to $2\pi$) of the oscillation. The abscissa represents the time scale $L/(U_0)_{\tilde{p}_{max}}$) of the mean flow through the cavity at maximum pressure amplitude. At worst, the deviation from $2n\pi$ is 2·4 %. So the existence of a 'phase core' through the central portion of the jet has provided us with the remarkably simple relation of $2n\pi$, compared to $(n+a)\,2\pi$ (where $a$ is an empirically determined constant) reported for a variety of impinging flows involving measurements *within* the unstable laminar shear layers, as reviewed

by Rockwell & Naudascher (1979), Hussain & Zaman (1978*a*), and Karamcheti *et al.* (1979).

The close relation between phase deviation $\phi_{\tilde{u}_L} - \phi_{\tilde{u}_0} - 2n\pi$ and pressure amplitude $\tilde{p}$ is further underscored in figure 4(*d*). For the case $(U_0)_{\tilde{p}_{max}} = 14{\cdot}4$ m/s, $L/D = 2$, changes in $\Delta\phi = \phi_{\tilde{u}_L} - \phi_{\tilde{u}_0}$ with $U_0 - (U_0)_{\tilde{p}_{max}}$ are large, and the corresponding variation in $\tilde{p}$ is also large. However, for the case $(U_0)_{\tilde{p}_{max}} = 17{\cdot}2$ m/s, $L/D = 2$, $\Delta\phi$ changes relatively slowly with $U_0$; likewise, the pressure $\tilde{p}$ is also varies slowly. The values of the '$Q$ factor' corresponding to these two cases are respectively 14·2 and 5·2, where $Q = \omega_n/(\omega_1 - \omega_2)$ is indicative of damping of the acoustic mode; maximum pressure amplitude is defined to occur at $\omega_n$, and 0·707 times the maximum amplitude at $\omega_1$ and $\omega_2$. As will be shown by measurements at $x/L \simeq 0$, the hydrodynamic (instability) and acoustic contributions to the organized wave are nearly equal for the case $(U_0)_{\tilde{p}_{max}} = 14{\cdot}4$ m/s, $Q = 14{\cdot}2$; on the other hand, the hydrodynamic (instability) contribution is nearly four times the acoustic contribution for the case $(U_0)_{\tilde{p}_{max}} = 17{\cdot}2$ m/s, $Q = 5{\cdot}2$. These relative amplitudes of instability and acoustic waves are central to understanding the amplitude and phase distributions of the resultant organized wave.

## 5. Amplitude and phase distributions of organized wave

Streamwise distributions of velocity amplitude and phase of the organized wave for the two representative cases of figure 4(*d*) are shown in figures 5 and 6. The curve parameter is deviation from the value of phase difference giving maximum pressure amplitude in the cavity $\{(\phi_{\tilde{u}_L} - \phi_{\tilde{u}_0}) - (\phi_{\tilde{u}_L} - \phi_{\tilde{u}_0})_{\tilde{p}_{max}}\}$; it can be related to mean velocity $U_0$ via figure 4(*d*). The ratio of instability to acoustic-wave amplitude at $x \simeq 0$ is represented by $|F/D_1|$. The case of figure 5(*a*) not only has a Strouhal number $S_D$, but also growth and overall amplification of fluctuation velocity $\tilde{u}(x)/U_0$, remarkably similar to the externally excited jet of Crow & Champagne (1971); consequently it serves as a convenient reference case.

Amplitude distributions shown in figures 5(*a*, *b*) exhibit features not obvious in studies involving relatively low-level loudspeaker excitation of laminar shear layers (e.g. Freymuth 1966) or purely hydrodynamic (in water) self-sustained oscillations of impinging free shear layers (Knisely & Rockwell 1982). In these cases, the disturbance undergoes an exponential amplification soon after separation, while the distributions of figure 5 exhibit no comparable growth region for $x \lesssim 0{\cdot}35D$; rather, the apparent amplitude tends to remain constant (figure 5*a*) or even decrease (figure 5*b*) with streamwise distance in the near field. These near field trends have been observed for axisymmetrically excited ($m = 0$ mode) jets by Pfizenmaier (1973) and Davies (1977), who proposed corresponding superposition models in the spirit of Ronneberger (1967), and by Hussain & Zaman (1978*a*) for laminar initial conditions, as well as by Crow & Champagne (1971), Chan (1974), and Moore (1977) for turbulent initial conditions.

Furthermore, in figure 5(*b*), where the instability and acoustic waves have nearly the same amplitude $|F/D_1| \simeq 1$, the initial decrease in organized-wave amplitude is followed by a series of peaks and valleys, resembling a quasi-standing-wave pattern. The wavelength of this pattern is of the order of the cavity inlet diameter $D$, whereas the corresponding acoustic wavelength $\lambda_a \gtrsim 25D$.

These features described in figures 5(*a*, *b*) may be modelled as follows. Considering

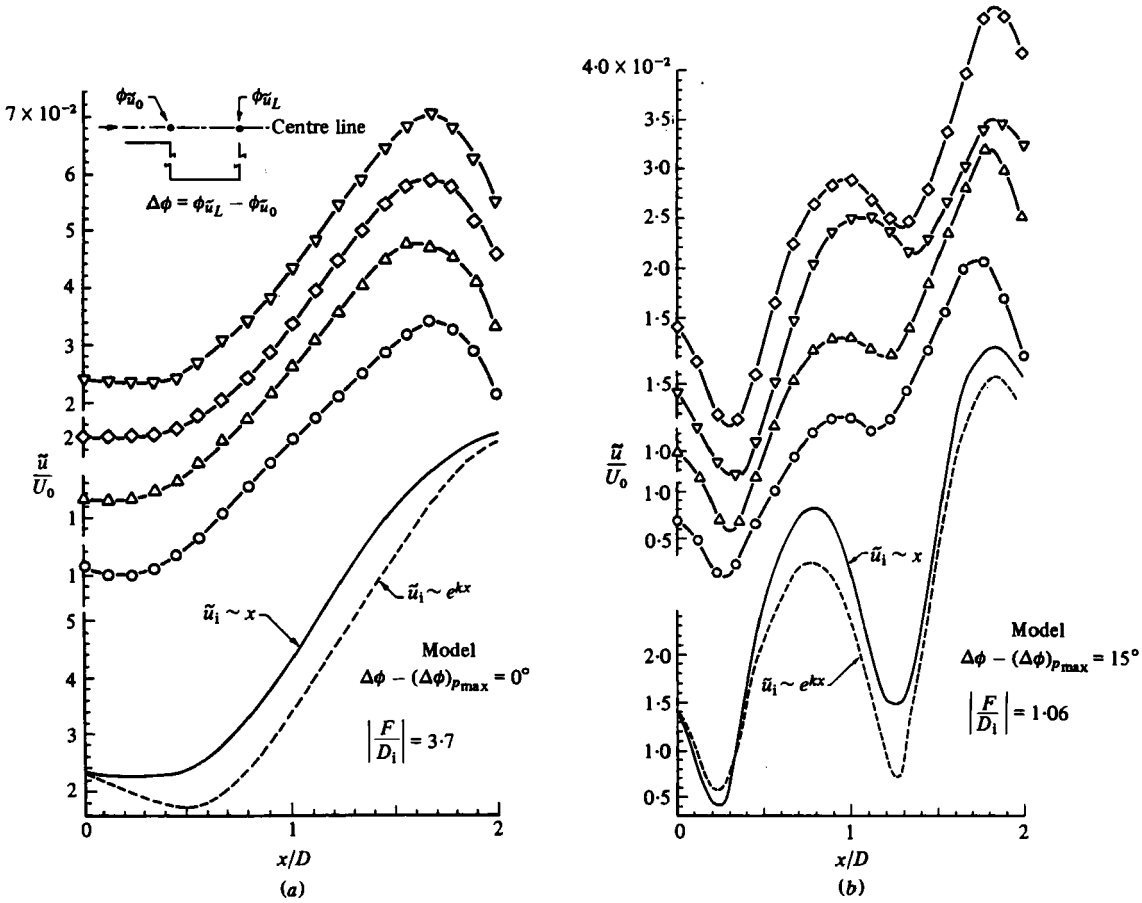


FIGURE 5. (*a*) Distribution of organized-wave amplitude along centre-line ($\tilde{u}/U_0$) for instability wave-dominated oscillation ($Re_{\theta_0} = 2{\cdot}6 \times 10^3$, $L/D = 2$, $|F/D_i| \simeq 4$). Curve parameter is deviation of phase difference of centre-line velocity ($\Delta\phi = \phi_{\tilde{u}_L} - \phi_{\tilde{u}_0}$) from that value producing maximum organized pressure amplitude ($(\Delta\phi)_{\tilde{p}_{max}} = (\phi_{\tilde{u}_L} - \phi_{\tilde{u}_0})_{p_{max}}$): ▽, $\Delta\phi - (\Delta\phi)_{\tilde{p}_{max}} = 0°$; ◇, 12°; △, 20°; ○, 22°. (*b*) Distribution of organized-wave amplitude along centre-line for acoustic wave and instability wave having nearly equal amplitudes ($Re_{\theta_0} = 2{\cdot}2 \times 10^3$, $L/D = 2$, $|F/D_i| \simeq 1$); ▽, $\Delta\phi - (\Delta\phi)_{\tilde{p}_{max}} = -26°$; ◇, −17°; △, 6°; ○, 15°.

the velocity field $\tilde{u}_1(x)$ of the organized wave pattern to be due to a one-dimensional, downstream propagating, 'instability' ($F$) wave, and upstream and downstream travelling acoustic ($D$) waves, having complex amplitudes $F = F_R + iF_I$ and $D = D_R + iD_I$ respectively, the imaginary and real components of the resultant wave pattern, obtained by superposition, can be written as

$$\left(\frac{\tilde{u}}{D_I}\right)_I = 2\cos k_a x + \frac{F_I}{D_I}\cos k_1 x - \frac{F_R}{D_I}\sin k_1 x \tag{1a}$$

$$\left(\frac{\tilde{u}}{D_I}\right)_R = \frac{F_R}{D_I}\cos k_1 x + \frac{F_I}{D_I}\sin k_1 x, \tag{1b}$$

in which $k_1$ and $k_a$ are the wavenumbers of the instability and acoustic waves. Although

$D_I$ may be approximated as independent of $x$, $F$ is a function of $x$, thereby accounting for streamwise amplification of the instability wave. Values of $F_R$, $F_I$, and $D_I$ at $x = 0$ were determined by two sets of simultaneous pressure and velocity measurements, exploiting the fact that the ratio of acoustic to hydrodynamic (instability) pressure is large in this region. In short, the pressure tap nearest separation (see figure 1) was used as a reference in determining the magnitude of the acoustic velocity (accounting for up- and downstream travelling waves (Skudrzyk 1971, p. 296), and the phase and amplitude of the organized wave (due to acoustic and hydrodynamic contributions) at the centre-line of the pipe. Using complex decomposition, values of $F_R$, $F_I$ and $D_I$ were arrived at. Moreover, $k_a$ follows from knowledge of $\bar{c}$ and $f$; $k_1$ can be determined from instability theory (Michalke 1971) or the measured wavenumber $k_{ow}$ of the organized wave. That is, $k_{ow} = \frac{1}{2}(k_a + k_1)$. Concerning variation of the instability-wave amplitude with $x$, represented by $F(x)$, it is unknown *a priori*. Two extreme variations were assumed: exponential ($\tilde{u}_1 \sim F \sim \exp \alpha x$, $\alpha = \text{const.}$), and linear ($\tilde{u}_1 \simeq F \simeq x$), to account for the possibility that the wave amplitude grows non-exponentially owing to the relatively high $\tilde{u}_1$ at separation. As shown in figures 5 (*a*, *b*), the forms of the predicted distributions of the organized wave are relatively insensitive to the assumed variation of $F(x)$.

For the case of figure 5 (*a*), the region of constant, or slightly decreasing, wave amplitude $\tilde{u}$ immediately downstream of separation is well-predicted, emphasizing that such near-field distortions (within the jet core) are not necessarily due to spatial non-homogeneity of the developing hydrodynamic disturbance field (Crighton & Gaster 1976). Within the shear layer, such non-homogeneity of the hydrodynamic field has been effectively demonstrated via vortex-sheet representations of the shear layer (Orszag & Crow 1970; Crighton 1972); however, in experimental situations, presence of an acoustic wave may induce additional distortions, complicating interpretation of the degree of *apparent* non-homogeneity. Also important is the sign change in curvature of the predicted wave pattern for $x/D \lesssim 1{\cdot}5$. Since there is no sign change in curvature associated with the assumed amplitude distributions of the instability wave ($\sim \exp \alpha x$ and $\sim x$), presence of the acoustic wave is responsible for this distortion; consequently, what might be interpreted as an *apparent* onset of non-linear saturation of the instability (hydrodynamic) amplitude distribution measured for self- or externally excited jets can be influenced by superposition effects of acoustic and instability waves if the acoustic-wave amplitude is sufficiently large. The deviation of the model from data in the vicinity of impingement ($x = L$) may be due to the fact that the model does not account for the later stages of disturbance saturation. Concerning the case of figure 5 (*b*), the severe decrease in wave amplitude immediately downstream of separation is well modelled. In addition, the subsequent peak–valley pattern is well-represented by the curves corresponding to the model.

Despite the necessity of knowing streamwise distributions of phase in deducing local disturbance velocities, and in physically interpreting overall phase differences $\phi_{\tilde{u}_L} - \phi_{\tilde{u}_0}$ between separation and impingement for self-sustaining oscillations, attention has not been given to the possibility of a background acoustic wave distorting the phase distributions of the instability wave. Phase distributions corresponding to the amplitude distributions of figures 5 (*a*, *b*) are shown in figures 6 (*a*, *b*), with predicted variations determined from (1). Clearly, for the case of significant acoustic-wave amplitude (small values of $x/D$ in figure 6*b*), local phase velocities of the instability

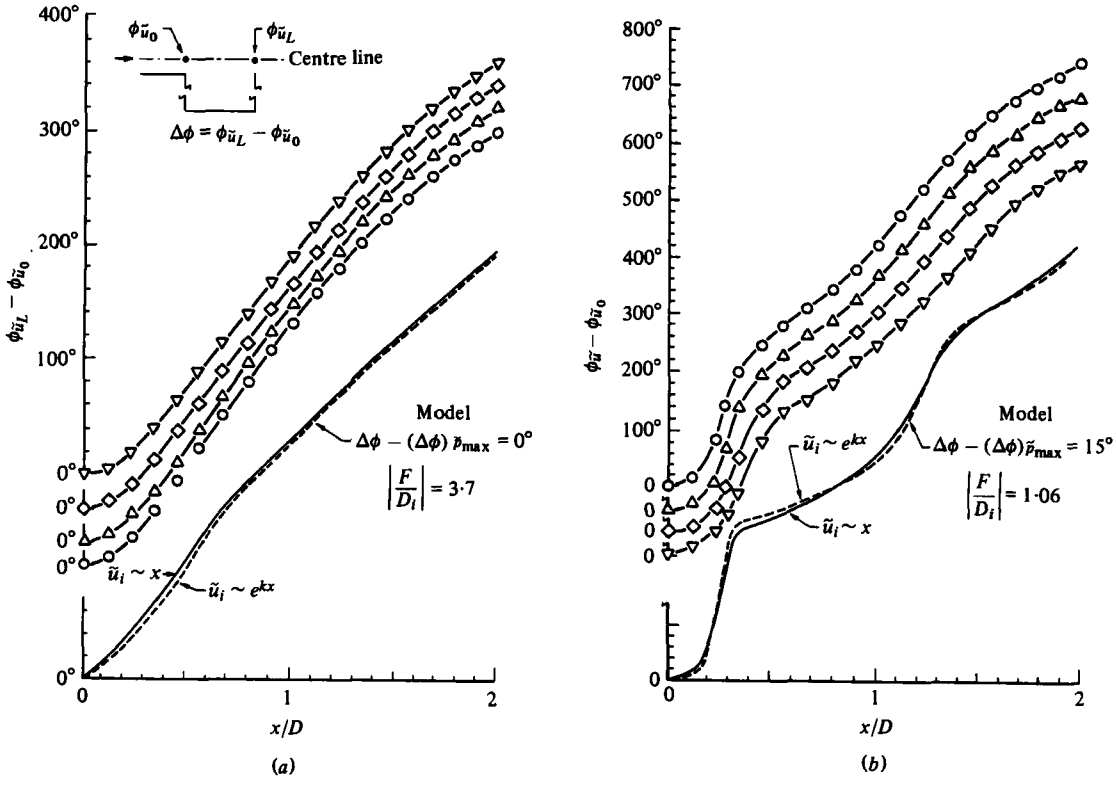


FIGURE 6. Phase distributions along centre line corresponding to cases (*a*) and (*b*) of figure 5. (*a*) ○, $\Delta\phi - (\Delta\phi)_{\tilde{p}_{max}} = 0$; △, 12°; ◇, 20°; ▽, 22°. (*b*) ○, 15°; △, 6°; ◇, −17°; ▽, −26°.

wave cannot be deduced accurately from measured distributions of phase of the organized wave.

With regard to the overall phase difference of the organized wave measured along the centre line (i.e. $\phi_{\tilde{u}_L} - \phi_{\tilde{u}_0} = 2n\pi$), previously discussed as a necessary condition for maximum-amplitude oscillations, it is important to point out that it holds irrespective of the degree of distortion of the streamwise phase distributions, for all cases given in figure 4(*c*). For purely hydrodynamic oscillations (i.e. completely dominated by the instability wave), this phase difference corresponds to $n$ equivalent wavelengths of the instability wave. However, presence of the background acoustic wave, even though its wavelength $\lambda_a$ is very long, requires careful interpretation of this phase difference. For example, if $\lambda_a \gg L$ (i.e. $k_a x_{max} \ll 1$), $k_i$ is assumed invariant with $x$, and $k_i x = 0, 2\pi, 4\pi, \ldots$ are taken to correspond to $0, 1, 2, \ldots$ wavelengths of the instability wave, then the phase difference between any downstream location where $k_i x = 2n\pi$ and separation where $k_i x = 0$ may be written as

$$(\phi)_{k_i x = 2n\pi} - (\phi)_{k_i x = 0} = 2n\pi + \arctan\{2D_I/F_R(x) + F_I(x)/F_R(x)\}_{k_i x = 2n\pi} - \arctan\{2D_I/F_R(x) + F_I(x)/F_R(x)\}_{k_i x = 0}, \quad (2)$$

in which the term $2n\pi$ on the right-hand side of (2) accounts for zero-crossings of $\phi(x)$. The ratio $F_I(x)/F_R(x)$ is constant if the phase of the complex modulus of the instability wave $F$, relative to the acoustic wave, is constant. Consequently, the organized-wave

phase difference $\phi_{\tilde{u}_L} - \phi_{\tilde{u}_0} = 2n\pi$ can be interpreted as the phase difference due to the instability wave only if the amplitude $D_I$ of the acoustic wave is very small compared to the real part $F_R(x)$ of the instability wave.

## 6. Conclusions

The highly coherent oscillations observed herein can be characterized in terms of an organized wave, having acoustic- and hydrodynamic- (instability-) wave components. If the acoustic wave(s) has a sufficiently large amplitude, the organized wave distribution can be substantially distorted, resulting in streamwise variations of amplitude and phase quite unlike what one would expect from consideration of only the instability wave. The distortion can complicate interpretation of spatial non-homogeneity of the developing instability wave (imposed by the solid separation boundary), onset of nonlinear saturation of the instability-wave amplitude, and local streamwise phase gradients (essential for determining local phase speeds of the instability wave).

Concerning the phase difference of the organized-wave velocity fluctuations between separation and impingement, it satisfies the condition of $2n\pi$ (measured within the core of the jet) when the pressure amplitude within the cavity takes on its maximum value. This relation holds for all cases examined, regardless of the degree of distortion of the organized wave by the acoustic-wave component. However, this phase difference deviates from what would be predicted from strictly hydrodynamic conditions if the amplitude of the acoustic wave becomes sufficiently large.

The authors wish to express their gratitude to Mr Gregory Gates, who assisted in some of the data reduction. This investigation was made possible by the financial support of the National Science Foundation of Washington, D.C. and the Volkswagen Foundation of Hannover, West Germany.

## REFERENCES

ARCHIBALD, F. S. 1975 Self excitation of an acoustic resonance by vortex shedding. *J. Sound Vib.* **38**, 81–103.

CHAN, Y. Y. 1974 Spatial waves in turbulent jets. *Phys. Fluids* **17**, 46–53.

CRIGHTON, D. G. 1972 Radiation properties of the semi-infinite vortex sheet. *Proc. R. Soc. Lond.* A **330**, 185–198.

CRIGHTON, D. G. 1975 Basic principles of aerodynamic noise generation. *Prog. Aero. Sci.* **16**, 31–96.

CRIGHTON, D. G. & GASTER, M. 1976 Stability of slowly diverging jet flow. *J. Fluid Mech.* **77**, 397–413.

CROW, S. C. & CHAMPAGNE, F. H. 1971 Orderly structure in jet turbulence. *J. Fluid Mech.* **43**, 547–591.

CUMPSTY, N. A. & WHITEHEAD, D. S. 1971 The excitation of acoustic resonances by vortex shedding. *J. Sound Vib.* **18**, 353–369.

DAVIES, P. O. A. L. 1977 Bench test procedures and exhaust system performance prediction. In *Proc. Surface Transportation Exhaust System Noise Symposium*. U.S. Environmental Protection Agency, EPA no. 550/9-78-206.

DAVIES, P. O. A. L. & YULE, A. J. 1975 Coherent structure in turbulence. *J. Fluid Mech.* **69**, 513–537.

ELDER, S. A. 1978 Self-excited depth mode resonance for a wall-mounted cavity in turbulent flow. *J. Acoust. Soc. Am.* **64**, 877–890.

FFOWCS WILLIAMS, J. E. 1969 Hydrodynamic noise. *Ann. Rev. Fluid Mech.* **1**, 197–222.

FREYMUTH, P. 1966 On transition in a separated laminar boundary layer. *J. Fluid Mech.* **25**, 683–704.

HASAN, M. A. Z. & HUSSAIN, A. K. M. F. 1979 A formula for resonance frequencies of a whistler nozzle. *J. Acoust. Soc. Am.* **65**, 1140–1142.

HILL, W. G. & GREENE, P. R. 1979 Increased turbulent jet mixing rates obtained by self-excited acoustic oscillations. *Trans. A.S.M.E.* I, *J. Fluids Engng* **99**, 520–525.

HO, C.-M. & NOSSIER, M. S. 1981 Dynamics of an impinging jet. Part 1. The feedback phenomenon. *J. Fluid Mech.* **105**, 119–142.

HUSSAIN, A. K. M. F. & ZAMAN, K. B. M. Q. 1978*a* Controlled perturbation of circular jets. In *Structure and Mechanisms in Turbulence* (ed. H. Fiedler), Lecture notes in Phys. vol. 75, pp. 31–42. Springer.

HUSSAIN, A. K. M. F. & ZAMAN, K. B. M. Q. 1978*b* The free shear layer tone phenomenon and probe interference. *J. Fluid Mech.* **87**, 349–383.

IBERALL, A. S. 1950 Attenuation of oscillatory pressures in instrument lines. *J. Res. Nat. Bureau of Standards* **45**, 85–94.

KARAMCHETI, K., BAUER, A. B., SHIELDS, W. C., STEGUN, G. R. & WOOLLEY, J. A. 1969 Some basic features of an edgetone flow field. *Basic Aerodynamic Noise Research*, NASA-SP-207, pp. 275–304.

KNISELY, C. & ROCKWELL, D. 1982 Self-sustained low-frequency components in an impinging shear layer. *J. Fluid Mech.* **116**, 157–186.

KIBENS, V. 1980 Interaction of jet flowfield instabilities with flow system resonances. *A.I.A.A.* 80–0963.

KO, N. W. M. & DAVIES, P. O. A. L. 1971 The near field with the potential core of subsonic cold jets. *J. Fluid Mech.* **50**, 49–78.

LAU, J. C., FISHER, M. J. & FUCHS, H. V. 1972 The intrinsic structure of turbulent jets. *J. Sound Vib.* **22**, 379–406.

LAUFER, J. 1953 The structure of turbulence in fully developed pipe flow. *N.A.S.A. Rep.* no. 1174.

MAESTRELLO, L. & FUNG, Y.-T. 1979 Quasi-periodic structure of a turbulent jet. *J. Sound Vib.* **64**, 107–122.

MICHALKE, A. 1965 On spatially growing disturbances in an inviscid shear layer. *J. Fluid Mech.* **23**, 521–544.

MICHALKE, A. 1971 Instabilität eines Kompressiblen runden Freistrahls unter Berücksichtigung des Einflusses der Strahlgrenzschichtdicke. *Z. Flugwiss.* **8/9**, 319–328.

MOLLO-CHRISTENSEN, E. 1967 Jet noise and shear flow instability seen from an experimenter's viewpoint. *Trans. A.S.M.E.* E, *J. Appl. Mech.* **89**, 1–7.

MOORE, C. J. 1977 The role of shear layer instability waves in jet noise. *J. Fluid Mech.* **80**, 321–367.

ORSZAG, S. A. & CROW, S. C. 1970 Instability of a vortex sheet leaving a semi-infinite plate. *Stud. Appl. Math.* **49**, 167–181.

PARKER, R. 1966 Resonance effects in wake shedding from parallel plates; some experimental observations. *J. Sound Vib.* **4**, 62–72.

PFIZENMAIER, E. 1973 On the instability of a sound influenced free jet. *E.S.R.O. Tech. Transl.* no. 122 (Transl. of *DFVLR Berlin Rep.* DLR-FB 73–69).

PLASCHKO, P. 1979 Helical instabilities of slowly divergent jets. *J. Fluid Mech.* **92**, 209–215.

ROCKWELL, D. 1977 Prediction of oscillation frequencies due to unstable flow past cavities. *Trans. A.S.M.E.* I, *J. Fluids Engng* **99**, 294–300.

ROCKWELL, D. 1982 Oscillations of impinging shear layers. Invited lecture, 20th A.I.A.A. Aerospace Sciences Meeting, 11–13 January. *A.I.A.A. Paper* no. 82-0047.

ROCKWELL, D. & KNISELY, C. 1979 The organized nature of flow impingement upon a corner. *J. Fluid Mech.* **93**, 413–432.

ROCKWELL, D. & NAUDASCHER, E. 1979 Self-sustained oscillations of impinging free shear layers. *Ann. Rev. Fluid Mech.* **11**, 67–94.

ROCKWELL, D. & SCHACHENMANN, A. 1979 A quasi-standing-wave phenomenon due to oscillating internal flow. *A.S.M.E. Paper* no. 79-WA/FE-24. *Trans. A.S.M.E.* I, *J. Fluids Engng* (to be published).

RONNEBERGER, D. 1967 Experimentelle Untersuchungen zum akustischen Reflexionsfaktor um unstetigen Querschnittsänderungen in einem Luftdurchströmten Rohr. *Acustica* **19**, 222–235.

SCHACHENMANN, A. & ROCKWELL, D. 1980 Self-sustained oscillations of turbulent pipe flow terminated by an axisymmetric cavity. *J. Sound Vib.* **73**, 61–72.

SKUDRZYK, E. 1971 *The Foundation of Acoustics.* Springer.

TAM, C. K. W. & BLOCK, P. T. W. 1978 On the tones and pressure oscillations induced by flow over rectangular cavities. *J. Fluid Mech.* **89**, 373–399.